Temperature Sensing and Modeling Based on Optical Fiber Using the OFDR Technique

Leonardo Santos Magalhães[1*], Rafael Andrade Vieira[1], Bianca Kurihara Yoshii[1], Valmara Silveira Ponte[1], Milena Ventura Castro Meira[2], Lucas Cruz da Silva[1], Valeria Loureiro da Silva[1]

[1] *SENAI CIMATEC University Center, Optics and photonics engineering laboratory, Salvador, Bahia, Brazil*

[2] *Universidade Federal da Bahia (UFBA), Physics Institute, Salvador, Bahia, Brazil*

**SENAI CIMATEC; Leonardo.magalhaes@fbter.org.br*

Abstract: Optical Frequency Domain Reflectometry (OFDR) is a distributed sensing technique that stands out for its high spatial resolution and sensitivity, being widely applied in explosive risk environments, high temperatures, and high electromagnetic interference. The present work proposes a distributed temperature sensing system based on optical fiber using the OFDR technique, with the objective of visually modeling the thermal distribution of objects in real time. The system consisted of calibrating the sensor for the clear curve type optical fiber, which was separated into continuous segments and connected to an OFDR interrogator, allowing the collection of thermal data. A system was developed to process the data and generate a two-dimensional visual model based on the temperature distribution along the fiber. The results demonstrate that the system was able to identify thermal variations, with sensitivity and high spatial resolution, allowing the reconstruction of objects in contact with the fiber.

Keywords: OFDR, Distributed Optical Fiber Sensor, Temperature Sensor, 2D Modeling

Abbreviations: OFDR, Optical Frequency Domain Reflectometry. RTDs, resistance temperature detectors. DTS, Distributed Temperature Sensing. FBG, Fiber Bragg Grating. EVA, Ethylene-Vinyl Acetate. LTS, Long Term Support. ROS, Robot Operating System. VRAM, Video Random Access Memory.

1. Introduction

Precise and real-time temperature monitoring is a critical component in the operation of modern industrial systems, particularly in sectors such as energy, aerospace, advanced manufacturing, and hazardous environments like refineries and high-voltage equipment. While conventional temperature sensors, such as thermocouples and resistance temperature detectors (RTDs), remain widely used, they are often limited in their spatial resolution, electromagnetic compatibility, and ability to operate in harsh or distributed environments. Over the past four decades, fiber optic sensors have emerged as a compelling alternative, offering immunity to electromagnetic interference, chemical resistance, and the ability to be embedded within structures with minimal physical intrusion (Bos et al. 2013 [1]).

There are several techniques used for temperature sensing using optical fibers as a reliable and safe source for sensing in challenging environments, as shown by Mihailov SJ et al 2012 [2]. The most common are those based on Raman scattering (DTS), Brillouin scattering, and Bragg gratings (FBG), each technique presenting a specific advantage in terms of range and sensitivity.

The introduction of Optical Frequency Domain Reflectometry (OFDR) marked a turning point in distributed fiber sensing. Unlike time-domain methods, OFDR utilizes Rayleigh backscattering and correlates the reflected spectral signal with a reference trace, achieving sub-millimeter spatial resolution. Its advantages over conventional techniques for distributed temperature sensing are emphasized in the study by Liang C et al. 2021 [3], which highlights OFDR as a more promising technique.

This approach enables precise analysis of wavelength shift, spatial distribution, and attenuation characteristics along the optical fiber, as shown by Eickhoff W et al. 1981 [4]. The present work introduces a novel method for correlating temperature variations with shape modeling, using wavelength shift data acquired through the OFDR technique. In this way, it presents an implementation of distributed temperature sensing but also broadens its applicability to complex geometric reconstructions.

2. Methodology

2.1. Materials and Equipment

The development of the distributed temperature sensor integrated with a visual modeling interface, was carried out in two main stages: the calibration of the optical fiber and the implementation of a computational model in Python, designed to simultaneously reconstruct both the shape and temperature distribution of the object under analysis. For the object modeling process, the experimental set up included an OFDR interrogator (manufacturer: Luna Innovations, model: ODISI 6101) to acquiring the wavelength shift along the fiber in real time; a clear curve optical fiber (Corning Inc), selected for its low optical power attenuation under both micro and macrobending conditions; a soft EVA surface positioned beneath the fiber to minimize undesired mechanical strain. The assembly was mounted on a vibration-isolated optical table to ensure measurement stability (Figure 1). A computer running Ubuntu 22.04 LTS, chosen for its compatibility with ROS 2 Humble, and equipped with a dedicated graphics card with 2 GB of VRAM, executed the visual modeling algorithms responsible for reconstructing the object's geometry and temperature distribution.

Figure 1. Schematic assembly diagram.

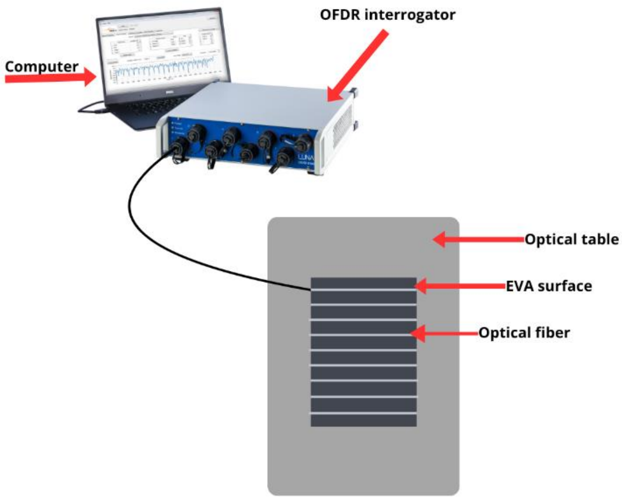

OFDR, Optical Frequency Domain Reflectometry.

2.2. Experiment Setup

The experimental configuration comprised a clear curve optical fiber in a serpentine coiled arrangement, on the EVA surface, as depicted in Figure 2. This layout preserved fiber continuity and allowed its division into 20 segments of approximately 13.5cm along the horizontal axis, which results in a spatial resolution of 1cm, in the vertical axis, calculated by dividing the height of the rectangular sensing region by the number of vertical fiber sections.

Figure 2. Temperature sensor setup. Fiber divided into 20 segments.

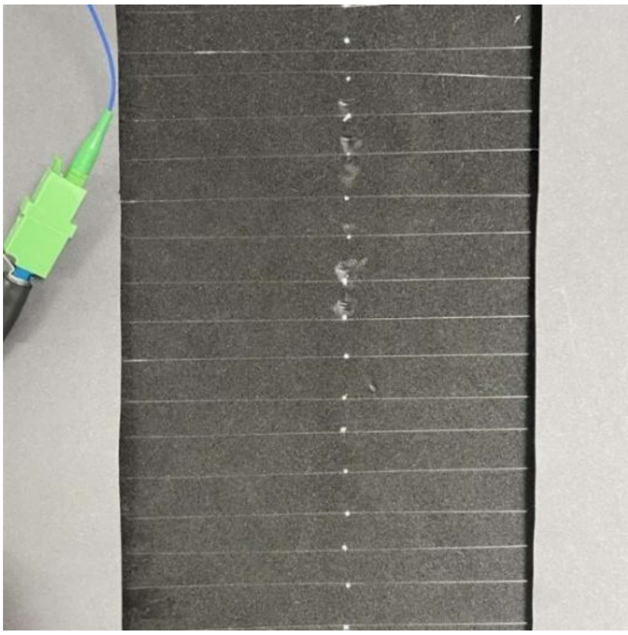

Following the system assembly, the fiber was connected to the OFDR interrogator enabling the acquisition and real-time transmission of sensing data across a network. Spectral shift measurements were sampled at intervals of 0.65 mm, corresponding to the spatial resolution along the horizontal axis as defined by the interrogator configuration.

2.3. Fiber Optic Calibration

The optical fiber was calibrated to determine the relationship between wavelength shift and temperature variation, ensuring reliable distributed thermal measurements. The procedure involved positioning the clear-curve optical fiber in a coil arrangement over a heated plate and applying controlled temperature increments from 20 °C to 100 °C in steps of 10 °C. A precision thermocouple monitored the surface temperature, while the OFDR interrogator simultaneously recorded Rayleigh backscattering traces. At each temperature step, multiple spectral shift datasets were collected at fixed spatial intervals. To ensure reproducibility, the calibration process was repeated three times. Data averaging was implemented through a Python algorithm to extract representative spectral shifts and perform linear regression against temperature. The resulting calibration curve defined the thermal sensitivity coefficient which directly relates temperature variation to the wavelength shift. The regression analysis yielded the following equation for the calibration line:

$$y = -0.761x + 19.7 \qquad (1)$$

where y is the temperature variation (°C) and x is the spectral shift (cm^{-1}), as shown in the graph in Figure 3.

Figure 3. Linear regression graph between temperature and spectral shift of an optical fiber.

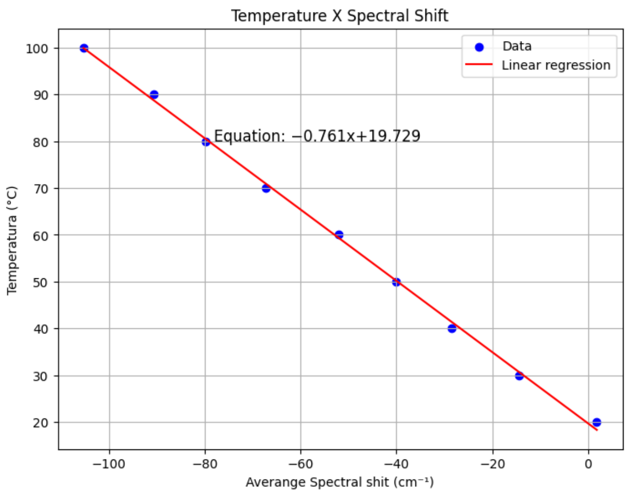

This calibration law was adopted as the reference for all subsequent temperature measurements in this work. The methodology demonstrated robustness, reproducibility, and high spatial resolution, confirming the suitability of OFDR-based sensing for distributed temperature monitoring. For a comprehensive description of the experimental setup, data acquisition procedures, and computational processing, readers are referred to Magalhães L et al. 2025 [5].

2.4. Procedures

A Python code was developed to process the spectral shift data, compute distributed temperature fields, and construct the geometric and thermal model of the analyzed objects. The algorithm begins by aligning the actual centers of the fiber segments with their corresponding assumed positions along the horizontal axis. This step compensates for minor displacements introduced during the fiber's installation, typically due to variations in mechanical tension or imprecise placement, which may result in misalignment between the physical and modeled fiber positions.

Based on a reference ambient temperature of approximately 20 °C, the algorithm renders the temperature distribution by mapping the spectral shifts observed along the 2.7 meter fiber segment. When heat is transferred to the fiber, a wavelength shift occurs due to fiber expansion. These shifts are continuously evaluated and visualized in real-time through a dynamic color map, where cooler regions are indicated in blue and warmer areas, typically reaching 35 °C or higher, are shown in red. The algorithmic workflow and data processing scheme are illustrated in Figure 4. This visualization enables simultaneous estimation of the distributed temperature profile and geometric reconstruction of the object based on the fiber's spatially resolved thermal response.

Figure 4. Block diagram of the system of the main algorithmic flows and solution structure.

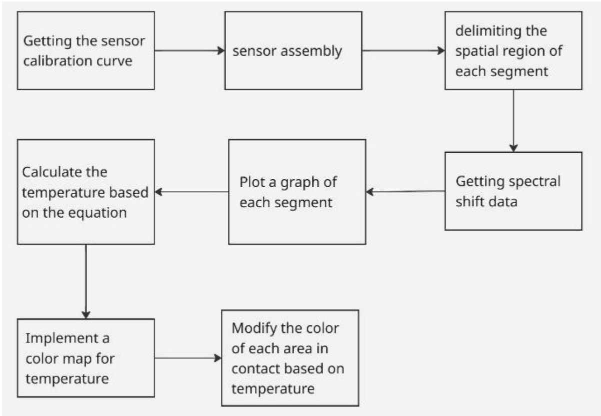

To evaluate system performance, experimental tests were performed using three different objects: a copper wire, a roll of copper tape, and a hand (Figure 5 to Figure 7). Each object was placed unheated and heated on the sensor to evaluate its modeling capability and distributed temperature mapping.

Initially, an unheated copper wire was arranged in an "S"-shaped configuration to assess the sensor's sensitivity to thin objects with low temperature variation and negligible weight.

Afterwards, a copper tape roll at room temperature was placed on the sensor to assess the influence of its weight on the measurement. The same roll was later uniformly heated with a heat gun and positioned again on the fiber, allowing evaluation of the response to an object with high curvature and increased cross-sectional area.

Finally, a human hand was gently placed over the sensor without exerting pressure, in two conditions: first at room temperature and then warmed through friction. This test examined the system's ability to detect differences of temperature distribution in objects with irregular geometry and non-uniform thermal gradients.

Figure 5. Unheated copper wire placed on the sensor

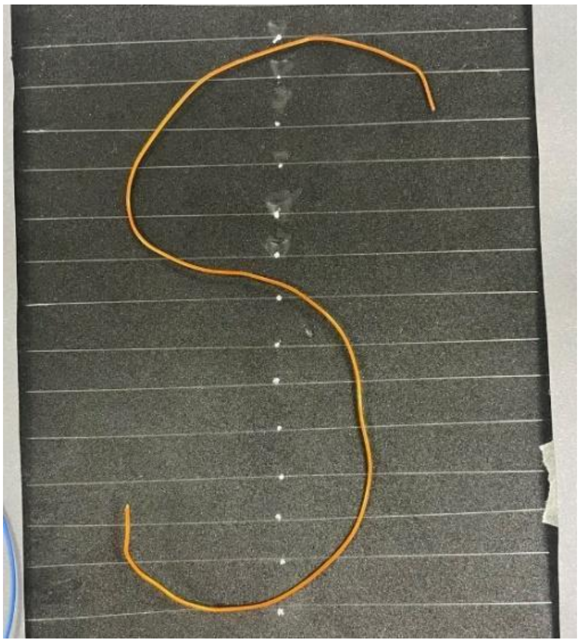

Figure 6. Heated copper tape placed on the sensor

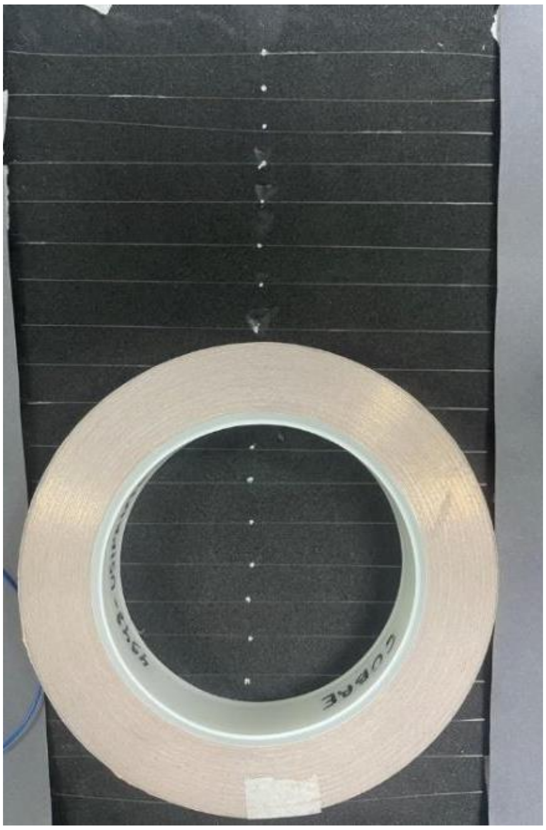

Figure 7. Heated hand placed on the sensor

3. Results and discussion

The use of OFDR as a thermal sensing technique has been previously demonstrated in the literature by Kreger ST et al. 2006 [6]. However, unlike the approach reported in that study, the present work proposes an implementation that extends beyond distributed temperature measurement along the fiber, enabling simultaneous two-dimensional shape reconstruction and spatially resolved thermal mapping of the contacted object.

Figure 8 through Figure 11 presents the final output generated by the modeling algorithm. Upon interaction with each object, the system produces a visualization of both the object's two-dimensional shape and its corresponding temperature distribution, while also providing the average temperature across the sensor's contact area. Figure 8 and Figure 9 demonstrate the sensor's sensitivity, as evidenced by its ability to detect subtle temperature variations. When analyzing the modeling of the unheated copper wire (Figure 8) and the unheated hand (Figure 9), measurable temperature variations were observed. This occurs because the copper wire, being a good thermal conductor, even without intentional heating, acquired residual heat during handling, contributing to the sensor response. Moreover, the human body temperature is higher than the reference temperature, which is sufficient to elicit a detectable spectral shift in the fiber.

The effect of strain induced by the object's weight was negligible in the present configuration. This occurs because the OFDR interrogator was specifically calibrated for temperature measurements, which alter the sensitivity coefficients used to interpret the spectral shifts. In this calibration mode, the coefficient applied for thermal sensitivity is expressed as:

$$y = -0.638\,x \qquad (2)$$

Whereas the coefficient associated with strain response is approximately ten times higher:

$$y = -6.67x \quad (3)$$

Consequently, the sensor becomes far less responsive to strain, rendering its contribution insignificant in the final output. This effect was confirmed in the case of the unheated copper tape roll, which, when placed on the fiber without prior handling, exhibited no measurable temperature variations and thus produced no detectable output. The same was observed when the copper wire was positioned without hand manipulation.

Figure 8. Sensor modeling with copper wire. Avenge temperature: 19.87º C

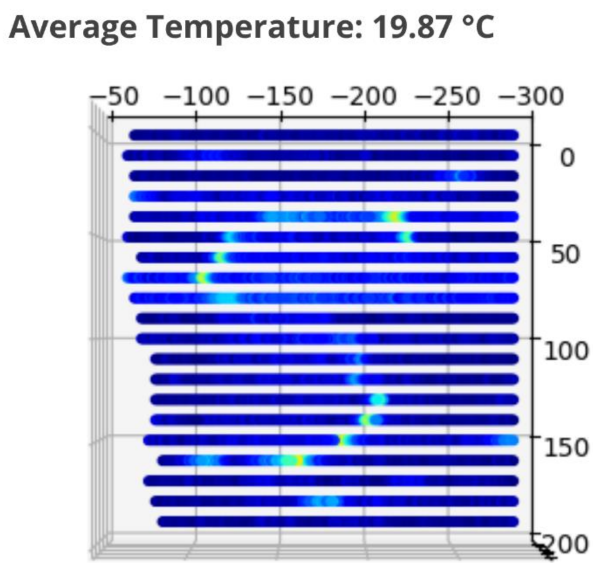

ISSN: 2357-7592

Figure 9. Sensor modeling of a non-heated hand. Avenge temperature: 20.52º C

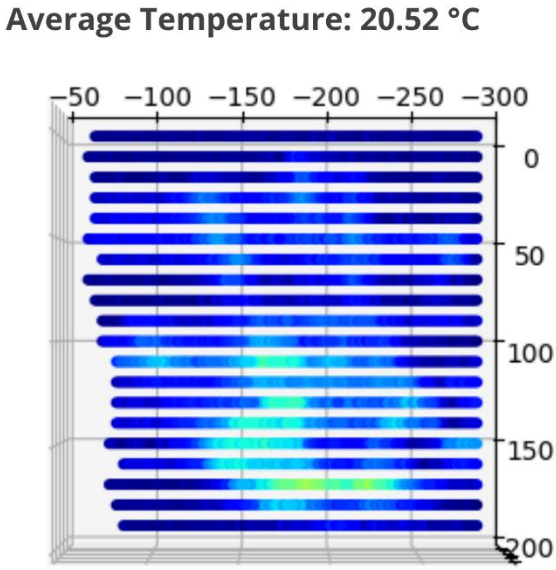

Figure 10. Sensor modeling of a hand heated by friction. Avenge temperature: 23.09º C

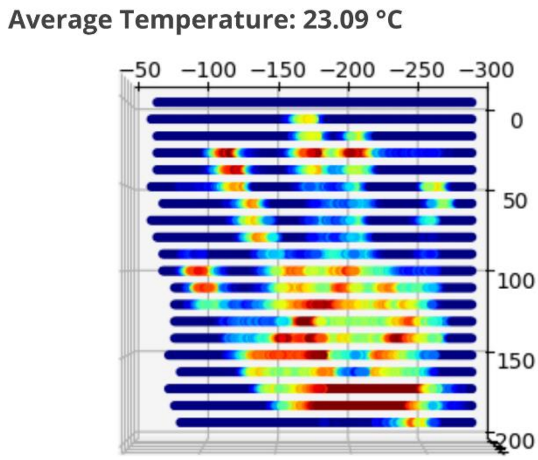

Figure 10 illustrates the high spatial resolution achieved by the proposed sensing system, demonstrating its ability to detect wavelength variations along the fiber with a sampling precision of 0.65 mm. This resolution enables accurate representation of detailed features of the object under study, facilitating the delineation of edges, contours, and subtle thermal variations.

When analyzing Figure 10, in which the human hand was heated by friction and gently placed over the sensor without applying pressure, the resulting thermal map faithfully reproduced the actual temperature distribution across the surface. Warmer regions correspond to areas of greater contact and pressure during friction, typically the more prominent parts of the hand, while cooler regions aligned with recessed zones, confirming the system's ability to resolve complex geometry with non-uniform thermal profiles.

Additionally, the technique shows potential for enhancement. By reducing the segment spacing along the vertical axis, the spatial resolution could be significantly improved, especially for objects with pronounced curvature. This limitation is evident in Figure 11, where the thermal modelling of a heated roll of copper tape reveals a loss of detail in the curvature representation due to insufficient vertical segmentation. Increasing the number of fiber segments would improve the resolution of the circular geometries, further demonstrating the capability of the OFDR technique, especially when integrated with the modelling framework proposed in this study.

Figure 11. Sensor modeling of heated copper tape. Avenge temperature: 23.65º C

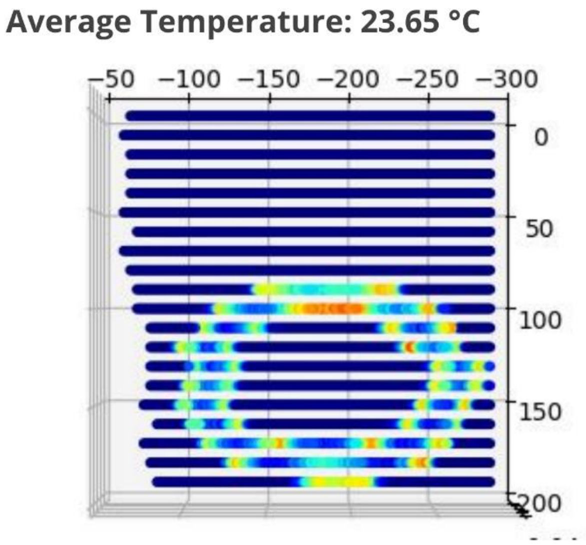

4. Conclusion

The development and implementation of a distributed thermal sensing system demonstrated promising results, both in terms of spatial resolution for shape modeling and thermal sensitivity. The experimental findings confirm the system's ability to simultaneously map two-dimensional object profiles and their corresponding real-time temperature distribution with considerable accuracy. Systematic testing with a copper wire, copper tape roll and human hand evidence its versatility: sensitivity to small conductive structures, ability to model bulkier curved objects, and robustness in capturing complex, non-uniform thermal fields in biological systems. The negligible contribution of strain, ensured by the calibration mode adopted, further reinforces the reliability of thermal measurements. The proposed approach expands the potential applications of sensing techniques, contributing to the advancement of OFDR-based technologies and establishing a foundation for future developments and enhancements.

Acknowledgement
The authors would like to thank CNPq, Shell Brazil Petróleo LTDA, the Brazilian Company for Industrial Research and Innovation (EMBRAPII), the Brazilian National Agency of Petroleum, Natural Gas and Biofuels (ANP), and Senai CIMATEC for their support and investments in Research, Development, and Innovation (R&D&I).

References

[1] Bos, J. J., Klein, J. W., Froggatt, M. E., Sanborn, E. E., & Gifford, D. K. (2013). *Fiber optic strain, temperature and shape sensing via OFDR for ground, air and space applications*. *8876*, 887614. https://doi.org/10.1117/12.2025711
[2] Mihailov SJ. Fiber Bragg Grating Sensors for Harsh Environments. Sensors. 2012 Feb 10;12(2):1898–918.
[3] Liang C, Bai Q, Yan M, Wang Y, Zhang H, Jin B. A Comprehensive Study of Optical Frequency Domain Reflectometry. IEEE Access. 2021;9:41647–68.
[4] Eickhoff W, Ulrich R. Optical frequency domain reflectometry in single-mode fiber. Applied Physics Letters. 1981 Nov 1;39(9):693–5.
[5] Magalhães Leonardo, Andrade Rafael, Ventura Milena, Loureiro Valeria. Calibração de sensor de temperatura distribuída de fibra óptica baseado em OFDR. 2025 Apr;1–3.
[6] Kreger ST, Gifford DK, Froggatt ME, Soller BJ, Wolfe MS. High Resolution Distributed Strain or Temperature Measurements in Single- and Multi-Mode Fiber Using Swept-Wavelength Interferometry. In: Optical Fiber Sensors. Washington, D.C.: OSA; 2006. p. ThE42.